J. Phys.: Condens. Matter **10** (1998) 8417–8428. Printed in the UK PII: S0953-8984(98)93030-2

Simulation studies of ZrW_2O_8 at high pressure

Alexandra K A Pryde†, Martin T Dove†§ and Volker Heine‡

† Mineral Physics Group, Department of Earth Sciences, University of Cambridge, Downing Street, Cambridge, CB2 3EQ, UK

‡ Cavendish Laboratory, University of Cambridge, Madingley Road, Cambridge, CB3 0HE, UK

Received 10 April 1998, in final form 13 July 1998

Abstract. The negative thermal expansion recently observed over a wide range of temperatures in the ambient pressure phase α-ZrW_2O_8 was attributed to the existence of low-frequency phonon modes which propagate with minimal distortion of the WO_4 tetrahedra and ZrO_6 octahedra, the so-called 'rigid unit modes'. The flexibility afforded this structure by these modes raises questions about the structure's behaviour with pressure. Further experiments found a high-pressure phase γ-ZrW_2O_8 which also exhibited negative thermal expansion. Calculations using the rigid unit mode model have shown that the mechanism described earlier in the context of α-ZrW_2O_8 is consistent with the negative thermal expansion in γ-ZrW_2O_8. Atomistic simulations have been used to calculate further properties of these two phases (e.g. transition pressure, compressibilities) using interatomic potentials derived for the earlier work on α-ZrW_2O_8. The reproduction of the cell parameters and bond lengths measured for γ-ZrW_2O_8 does not imply a substantial change in the bonding character of the W–O interactions.

1. Introduction

Recently Mary *et al* [1] reported the discovery of an isotropic negative thermal expansion in ZrW_2O_8 (cubic symmetry, space group $P2_13$). In two previous papers [2, 3] we proposed that this can be explained in terms of our 'rigid unit mode model' [4, 5]. The straightforward idea, put forward by Mary *et al* [1], is that transverse vibrations of the oxygen atoms in the Zr–O–W bonds will, by virtue of the relative stiffness of the Zr–O and W–O bonds, pull the Zr and W cations towards each other. Since the amplitude will increase with temperature, the effect will be an increased shrinkage on heating. The Zr–O and W–O bonds are not independent entities, but are parts of nearly rigid ZrO_6 octahedra and WO_4 tetrahedra respectively. Thus the idea translates easily into our rigid unit mode model, in which we consider the role of the thermal vibrations of a structure composed of rigid units that are linked together at their vertices. The rigid unit modes (RUMs) are the phonon modes that can propagate without the rigid units needing to distort. Since these will have low energy, their role in a wide range of phenomena can be highly significant. Our RUM model of thermal expansion is easily appreciated in figure 1, which shows a two-dimensional representation of a linked array of octahedra. The rotation of any octahedron will pull its neighbours inwards, causing a net reduction in volume. If this rotation is interpreted as a thermal vibration, with a mean-square rotation that is proportional to k_BT/ω^2, there will be a volume reduction that is proportional to this mean-square rotation. This argument has been developed and applied to the negative thermal expansion in β-quartz by Heine *et al* [6] and Welche *et al* [7].

§ To whom correspondence should be addressed.

0953-8984/98/388417+12$19.50

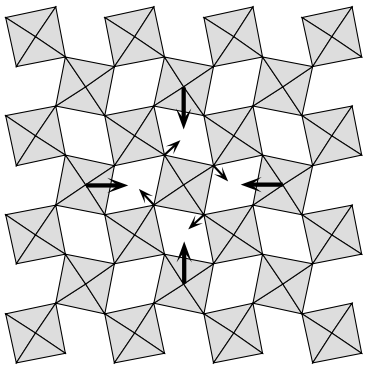

Figure 1. An arrangement of linked octahedra as found in the perovskite structure; the oxygen atoms form the corners of the octahedra. Rotation of one octahedron, as indicated by the arrows showing the movements of the oxygen atoms, causes the local environment to be pulled inwards, as shown by the bolder arrows marking the movements of the centres of the octahedra.

Although these ideas may appear at first sight to be almost intuitive, it is by no means obvious that any RUMs can exist in a given structure. In fact, the standard theoretical analysis used in the theory of glasses [8, 9] based upon the balance between the topological constraints and degrees of freedom (which, incidentally, was introduced by Maxwell in 1864 [10]) implies that there should be no RUMs in a structure such as ZrW_2O_8, which if true would invalidate both our specific RUM interpretation and the looser qualitative interpretation based only on transverse flexing of Zr–O–W bonds. However, we have shown elsewhere [4, 11] that when symmetry is properly taken into account there can be a small but non-zero number of RUMs or modes that are nearly RUMs (quasi-RUMs or QRUMs). Our previous papers [2, 3] showed that there are enough of these modes in ZrW_2O_8 to account for the negative thermal expansion, and we supported our theoretical analysis with lattice dynamics calculations of the thermal expansion based on a model interatomic potential. It should, however, be appreciated that the symmetry argument does not always allow for the existence of RUMs in structures containing linked polyhedra [12], and generally it only applies when there is an exact balance between the numbers of topological constraints and degrees of freedom, as in ZrW_2O_8, but not in the similar system ZrV_2O_7 [2]. The additional cross-bracing in this latter structure caused by the linkage of tetrahedra that is not present in ZrW_2O_8, as clearly seen in figure 2, is enough to destroy the RUM flexibility of the structure, so that all phonon modes must involve distortions of the polyhedra. This point is relevant when considering evidence for the formation of chemical cross-bracing in high-pressure phases.

Evans *et al* [13] have recently discovered a high-pressure phase of ZrW_2O_8 (γ-ZrW_2O_8) which also has negative thermal expansion. This phase is based on the ambient temperature/pressure α-phase, with a $1 \times 3 \times 1$ supercell and space group $P2_12_12_1$, figure 2. The structure of γ-ZrW_2O_8 is similar to that of α-ZrW_2O_8, but involves reorientations of some of the WO_4 tetrahedra, so cannot be obtained from α-ZrW_2O_8 by a simple displacive instability. The existence of this phase offers an opportunity to test the interpretation of the mechanism giving rise to negative thermal expansion. It also offers an opportunity to validate our model interatomic potential, which was derived using only a minimal amount of experimental data, and it is gratifying that our model is shown (below) to be able to reproduce the details of the structure of γ-ZrW_2O_8. Indeed, we are then able to use our

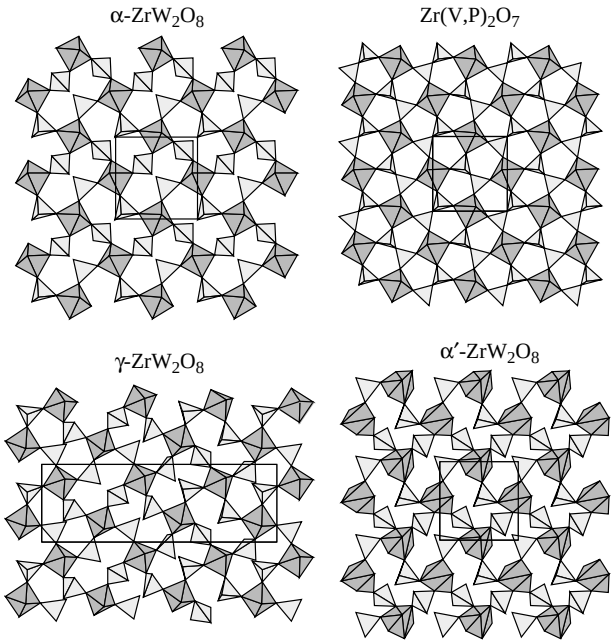

Figure 2. Comparison of the crystal structures of α-ZrW_2O_8, $Zr(V,P)_2O_7$, γ-ZrW_2O_8, and our proposed α'-ZrW_2O_8 (7 GPa), viewed down [001], showing the ZrO_6 octahedra (or ZrO_7 units) and WO_4 tetrahedra (lighter shading) as shaded polyhedra, all viewed down the [100] axis.

model to interpret some of the crystal-chemical aspects of the structure of this phase.

In this paper we will also show how the RUM model will apply to this new phase. It turns out that the basic RUM spectrum is barely altered by the existence of the phase transition, for reasons that are easily understood, but the greater compaction of the structure inhibits the amplitudes of the RUM fluctuations that give rise to the negative thermal expansion, so that the effect is smaller than in α-ZrW_2O_8. We can identify the specific details of the impaction of the structure that hinder the RUM amplitudes. The same model also explains why the bulk moduli of the two phases are very similar in magnitude.

As a postscript to this work, we also show that there are potential displacive instabilities of α-ZrW_2O_8 that could be induced by increasing pressure, which may be important in analogue materials in which the γ-phase does not have its own stability phase. At very high pressures we predict the possible stability of a new phase, which we denote as α' because it is based on the structure of α-ZrW_2O_8, and which has Zr in sevenfold coordination with oxygens. Because we have not searched for new phases in any systematic manner, we cannot predict whether some other phase will itself have lower energy than our proposed α'-phase, but we are able to predict that increasing pressure is more likely to produce new phases with distortions of the ZrO_6 octahedra rather than the WO_4 tetrahedra.

2. Calculations using a model interatomic potential for ZrW_2O_8

2.1. Description of the model

The calculations have used a model interatomic potential developed in our previous paper [2] and are based on the ionic model commonly used for the simulations of minerals and

ceramic oxides. Short-range interactions are assumed to follow the functional form

$$\phi(r) = B\exp(-r/\rho) - Cr^{-6}. \tag{1}$$

We assumed formal ionic charges, and modelled the polarizability of the O^{2-} anion with a shell model. The charge on the O^{2-} shell was $-2.848\,19$ electron units, and the core and the shell interacted through a harmonic potential in the core–shell separation u

$$\phi(u) = \tfrac{1}{2}ku^2. \tag{2}$$

We used the value $k = 74.92$ eV Å^{-2}. The spirit of the model as first introduced into the literature for oxides with tetrahedral coordination [14] is that the interatomic forces mostly interact through the shell rather than the core, but it is the position of the core that defines the position of the atom.

We also included bond-bending potentials for atoms within tetrahedra and octahedra that were of the form

$$\phi(\theta) = \tfrac{1}{2}K(\theta - \theta_0)^2. \tag{3}$$

The values used for the parameter K in the bond-bending potential were 0.4 and 0.5 eV for the O–Zr–O (equilibrium angle 90°) and O–W–O (equilibrium angle 109.47°) bonds respectively.

The values for the parameters in the shell model and for the short-range O...O potentials were taken from a good empirical model for SiO_2 [14] and were not modified in the present study. The remaining parameters (table 1 and above) were optimized for ZrW_2O_8 in our previous work [2] and the reader is referred there for further information. The optimization was based upon comparison of calculated and experimental crystal structures of α-ZrW_2O_8 at ambient pressure, together with information from the known vibrational frequencies of the WO_4 molecular ions in the mineral scheelite, $CaWO_4$. With additional information, such as the availability of the bulk modulus, or the structures of high-pressure phases [13], it should be possible to improve the model. This, however, is outside the scope of the present study.

Table 1. Values for the parameters of the short-range pair interactions in the model interatomic potential for ZrW_2O_8.

Ion pairs	B (eV)	ρ (Å)	C (eV Å^{-6})	Reference
W–O	1305.22	0.375	0.0	[2]
Zr–O	9×10^6	0.140	0.0	[2]
O–O	22764.0	0.149	27.879	[14]

Models such as the present model have been used with considerable success in the simulation of oxide minerals and ceramics over the past decade [15]. For aluminosilicates, bond lengths and lattice parameters can be predicted with an accuracy to within 2% and often values of the elastic constants can be predicted to within 10–20% [15]. These models have primarily been used for materials with tetrahedral and octahedral structural units, as in ZrW_2O_8, and they appear to capture most of the essence of the real forces in these materials.

In our previous study [2] our model was shown to give a reasonable prediction of the crystal structure of α-ZrW_2O_8 at ambient pressure. More strikingly, from calculations of the phonon spectra to give the crystal free energy, it was possible to calculate the thermal expansion, and the results were in remarkable agreement with the negative value obtained by experiment. With the availability of new high-pressure data [13], it is worth giving further evaluation of the model.

2.2. Simulation methods

We have performed two types of simulation with our model interatomic potential. In the first the lattice energy was minimized by relaxing the atomic positions and unit cell parameters starting from an assumed crystal structure, which is typically the experimental structure (the positions of the oxygen cores and shells were allowed to relax separately). At the point of lowest energy, information about structure and energies could be extracted. The second type of simulation involved calculations of phonon frequencies, both to calculate Grüneisen parameters and to calculate possible phonon instabilities (soft modes). All these simulations were performed using the GULP program [16]. One point to note is that in lattice energy relaxation calculations, the space group is constrained not to change; whilst it is possible for the structure to relax to a higher symmetry (parent space group), it is not possible for the structure to relax to a lower symmetry.

2.3. Calculation of the crystal structure of γ-ZrW_2O_8

The model interatomic potential was used to calculate the structure of γ-ZrW_2O_8 at zero pressure. Table 2 compares the observed [13] and calculated cell parameters of γ-ZrW_2O_8 and table 3 compares the observed [13] and calculated bond lengths. It is gratifying that our model, which was derived using only a minimal amount of experimental data, can reproduce the details of the structure of γ-ZrW_2O_8 reasonably well.

Table 2. Comparison of calculated and measured lattice parameters in α- and γ-ZrW_2O_8 (experimental data obtained at ambient pressure and temperature, calculations correspond to $T = 0$ K and $P = 0$ GPa).

	Observed (Å)	Calculated (Å)
a	9.067	9.082
b	27.035	27.069
c	8.921	8.881

In fact, the success of our model interatomic potential in reproducing the crystal structure of γ-ZrW_2O_8 actually gives us insights into the chemistry of this structure. In particular, if we focus on the W–O bond lengths, it can be seen that for each W atom there are four bonded O atoms with bond lengths of around 1.8 Å and in some cases there is another close O atom at a separation of around 2–2.4 Å. Evans *et al* [13] interpreted this as indicating the formation of additional W–O chemical bonds. The fact that our model has reproduced the same close distances without needing to invoke a separate interaction potential to do so (for example, we did not extend the three-body bond-bending potentials to these atoms) implies that there needs to be no new chemical bonding involved. Instead, the compactness of the structure of γ-ZrW_2O_8 forces the close separation of the W atoms and non-bonded O atoms, more in the sense of the packing of hard spheres than in the sense of forming new chemical bonds. This point is critical to understanding why negative thermal expansion is possible in γ-ZrW_2O_8—if additional cross-bracing chemical bonds were formed, the structure would not have enough flexibility to allow for the existence of RUMs (recall the discussion in section 1). Instead, the impaction of close oxygen atoms towards WO_4 tetrahedra may limit the amplitude of RUM rotations of the tetrahedra, which in turn will limit the size of the negative thermal expansion. We develop this discussion further below.

Table 3. Comparison of calculated and measured bond lengths in γ-ZrW_2O_8 (experimental data obtained at ambient pressure and temperature, calculations correspond to $T = 0$ K and $P = 0$ GPa). The fifth W–O distance given in some cases represents the closest non-bonded distances that Evans *et al* [13] have interpreted as actual chemical bonds.

	Observed (Å) [13]	Calculated (Å)
Zr1–O	1.975, 2.047, 2.055	2.125, 2.098, 2.099
	2.088, 2.090, 2.109	2.117, 2.157, 2.111
Zr2–O	1.953, 2.030, 2.055	2.113, 2.104, 2.100
	2.074, 2.125, 2.150	2.104, 2.115, 2.111
Zr3–O	1.979, 2.011, 2.023	2.093, 2.102, 2.090
	2.079, 2.096, 2.121	2.101, 2.107, 2.121
W1–O	1.712, 1.743, 1.855, 1.870	1.798, 1.750, 1.756, 1.760
	2.300	2.124
W2–O	1.739, 1.751, 1.792, 1.801	1.770, 1.763, 1.789, 1.758
	2.241	2.059
W3–O	1.777, 1.778, 1.792, 1.801	1.748, 1.764, 1.721, 1.755
W4–O	1.786, 1.791, 1.795, 1.825	1.748, 1.771, 1.770, 1.754
	2.341	2.375
W5–O	1.839, 1.855, 1.855, 1.861	1.774, 1.760, 1.808, 1.762
	2.181, 2.331	2.156, 2.447
W6–O	1.729, 1.798, 1.828, 1.870	1.742, 1.756, 1.773, 1.757
	2.394	2.189

2.4. Calculation of thermal expansion

In our previous study of α-ZrW_2O_8 the thermal expansion was calculated using a free-energy minimization method. When this method was applied to γ-ZrW_2O_8 it turned out to be impossible to obtain convergence of the minimized structure within a reasonable computing time and so we used the simpler method of calculating the thermal expansion of both α- and γ-ZrW_2O_8 (at both $T = 0$ K and $P = 0$ K, which are close to the experimental conditions of ambient temperature and pressure) through calculations of the phonon Grüneisen parameters [17]. The calculated value of the thermal expansion coefficient of γ-ZrW_2O_8 was -3.6×10^{-6} K^{-1}, which is close to the experimental value of -3.0×10^{-6} K^{-1} [13]. For comparison, our calculated value of the thermal expansion coefficient of α-ZrW_2O_8 calculated with the Grüneisen parameters is -24.6×10^{-6} K^{-1}, which is close to our previous value calculated by free-energy minimization methods [2] and close also to the experimental value of -26.4×10^{-6} K^{-1} [1, 13]. The fact that our model interatomic potential has reproduced the size of the negative thermal expansion coefficient of both phases of ZrW_2O_8 supports our argument above that we have properly captured the chemistry within the model, including the difference between real chemical W–O bonds and simple close W...O contacts arising from the impaction of the structure.

The way that the Grüneisen parameters scale with phonon frequency for a single wavevector is indicated in figure 3. It is clear from this figure that the low-frequency modes dominate the negative thermal expansion for both phases of ZrW_2O_8, consistent with our earlier analysis from the RUM model [2, 3].

2.5. Calculation of bulk modulus

Cell parameters and bond lengths for α- and γ-ZrW_2O_8 were calculated for a range of pressures, and the results were used to give the bulk modulus. For the two phases we

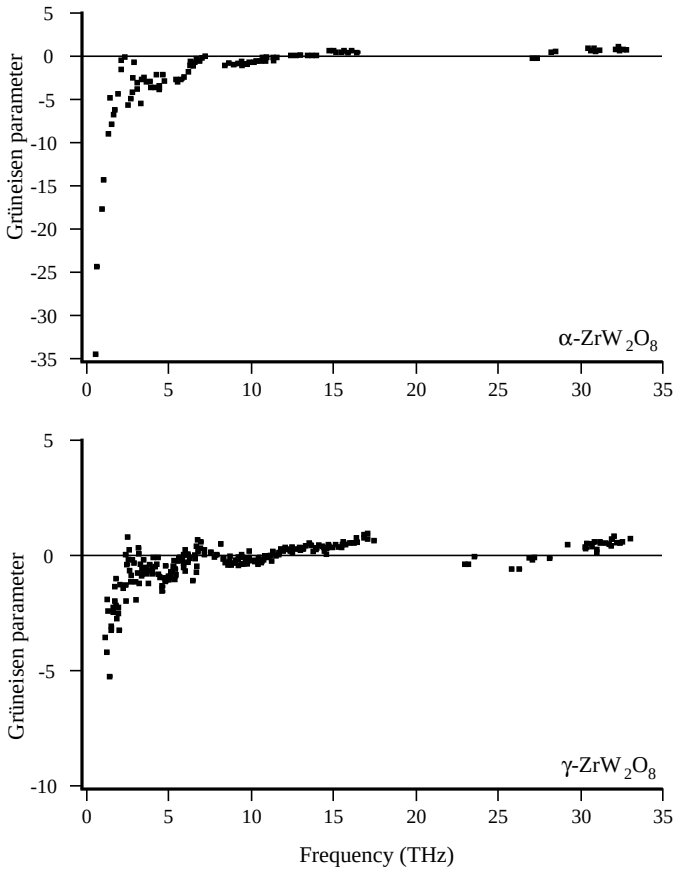

Figure 3. Calculated Grüneisen parameters for α-ZrW_2O_8 and γ-ZrW_2O_8 for the equivalent wavevectors $\boldsymbol{k} = (\frac{3}{8}, \frac{1}{8}, \frac{1}{24})$ and $\boldsymbol{k} = (\frac{3}{8}, \frac{3}{8}, \frac{1}{24})$ respectively, plotted as a function of phonon frequency.

obtained values of 0.59×10^{-2} (α) and 0.68×10^{-2} (γ), which are rather smaller than the experimental values of 1.44×10^{-2} (α) and 1.47×10^{-2} (γ) [13]. As noted above, the measured value of the bulk modulus, which was not available at the time of our earlier paper, could now be used to further optimize the model interatomic potential, but this is outside the scope of the present study. What is clear, however, is that our model gives very similar values for the bulk moduli of the two phases, exactly as found by experiment. We discuss this point further below.

2.6. Calculation of transition pressure and phase diagram

To determine a value for the critical pressure P_0 for the α–γ transition, the difference in the lattice enthalpy, ΔH, between the two phases at 0 K was calculated for a range of pressures. The solution of $\Delta H = 0$ gave $P_0 = -4.25$ GPa. At this pressure, the volume change, ΔV, associated with the transition was calculated to be 3% (compared with an experimental value of 5% [13]) and the lattice energy difference was -0.16 eV per formula unit. The difference in entropy of the two phases, ΔS, was calculated from the partition function using phonon frequencies calculated over a grid of wavevectors in reciprocal space.

Using the Clausius–Clapeyron equation the slope of the phase boundary in the P–T diagram for the system was determined as $\mathrm{d}P/\mathrm{d}T = \Delta S/\Delta V = 4.5$ MPa K^{-1} above 200 K. The resultant fixed point of the P–T diagram, i.e. $P_0 = -2.9$ GPa at $T = 300$ K, does not agree well with experiment, $P_0 = 0.2$ GPa [13]. This is actually a common problem in calculating pressure-induced phase transitions using empirical potentials, which arises from the fact that very small errors in the model interatomic potentials can be magnified to give large errors in calculated energy differences between two phases.

3. Rigid unit modes

As noted in section 1, the RUMs are the phonon modes that propagate without distortion of the linked polyhedra (in this case the WO_4 tetrahedra and ZrO_6 octahedra). If there are no forces other than those that maintain the rigidity of the polyhedra, the RUMs will have zero frequency and all other phonons will have frequencies that are determined by the extent to which the phonon eigenvectors required distortions of the polyhedra. We have developed a numerical method to calculate the zero-frequency RUMs for any general structure containing a framework of linked polyhedra [11]. In short, the essence of the approach is to represent each atom shared by two polyhedra (for example, at the corners) as a spring connecting two halves of a 'split atom', with equilibrium separation of zero. No other forces need to be used. The dynamical equations for this model give zero-frequency solutions for all RUMs. Formally, the size of the spring constants represents the stiffness of the polyhedra and it is tuned to give reasonable phonon frequencies for other phonon modes. This method has been programmed into our CRUSH program [11, 18]—see also [19]—and has been applied, among other things, to a number of studies of the phase stability in aluminosilicate minerals [4, 5] and to the issue of localized framework deformations in zeolites [20–22].

Using CRUSH we have calculated the RUM spectrum for γ-ZrW_2O_8. Since the basic topology of the structures of the γ- and α-phases is identical, it would be expected that the RUM spectrum should be the same in both cases and our results confirm this. In figure 4 we show the phonon density of states calculated for the two phases with our split-atom model [11]. The important point to note is that the calculated densities of states are very similar for both models, in particular that both have an excess of low-frequency modes down to zero energy above the normal Debye parabolic form. This is due to the RUMs and QRUMs described earlier (see [12] and also our earlier paper [2] on ZrW_2O_8 for comparisons of the computed density of states for examples with and without RUMs).

As noted above, an important result evident from the model calculations of the crystal structure of γ-ZrW_2O_8, table 3, is the good agreement between the calculated and the measured structures of γ-ZrW_2O_8. Since the model was derived using α-ZrW_2O_8, it only contains information relevant for WO_4 units. This implies that in the denser high-pressure γ-phase, the tungsten atoms remain fourfold coordinated and there is no change in their chemical bonding. Therefore we are suggesting that the structure is not cross-braced by additional W–O bonds as described by Evans *et al* [13], but that instead the structure is simply more impacted with additional interatomic contact between oxygen atoms. Were the structure of γ-ZrW_2O_8 to contain cross-bracing W–O bonds, this would remove a great deal of flexibility from the structure. For such a structure, in which no RUMs are permitted, the coefficient of thermal expansion according to our mechanism would be positive rather than negative. On the other hand, it is expected that the impaction to which we refer will inhibit the amplitude of some of the RUMs, and we suggest that this is the origin of the difference in the relative magnitudes of the two negative thermal expansion coefficients of α- and γ-ZrW_2O_8. Furthermore, the similarity of the observed and calculated bulk moduli

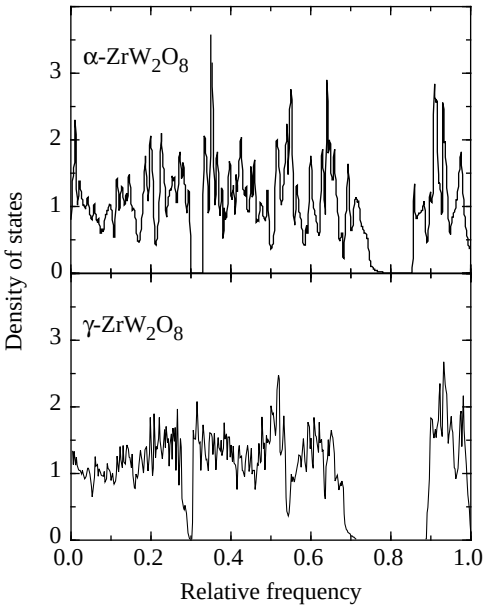

Figure 4. The vibrational density of states for α-ZrW_2O_8 and γ-ZrW_2O_8 calculated using our split-atom method. The RUM spectra are similar in many respects most notably that in both cases the density of states has a continuum of states at low frequencies arising from the RUMs and QRUMs present in both structures.

for the two phases given earlier is consistent with our view that there are no additional bonds between tungsten and oxygen atoms in the high-pressure phase cross-bracing the structure.

4. Other instabilities under pressure

4.1. Displacive (soft mode) instability

Our simulations of α-ZrW_2O_8 under pressure indicate that were this phase not to undergo the reconstructive transition to the γ-phase, it would develop soft modes associated with a displacive instability. The first mode to become soft under pressure falls to zero frequency at a pressure of $P_0 = 1.53$ GPa at the wavevector $\boldsymbol{k} \sim \boldsymbol{a}^*/10$, figure 5. The origin of a potential incommensurate instability is very similar to that of the actual incommensurate instability in quartz [23, 24]. An optic mode softens under pressure (this is the mode that is double-degenerate at $\boldsymbol{k} = 0$ in figure 5). This mode is actually soft across the whole branch for $\boldsymbol{k}$ along [100]. At $\boldsymbol{k} = 0$ the soft optic mode has a different symmetry to that of the acoustic modes. However, for a general $\boldsymbol{k}$ along [100] the symmetry of the soft optic mode is the same as that for one of the transverse acoustic modes, and as the frequency of the acoustic mode increases with $\boldsymbol{k}$ it will want to cross the optic branch in the dispersion curves. However, because the two modes are of the same symmetry they cannot actually cross, and the dispersion curves will 'repel' each other in a way that is seen as typical 'anti-crossing'. This is clearly seen in figure 5. The interaction that determines the size of the repulsion of the two phonon branches varies as k^2, and therefore increases for larger $\boldsymbol{k}$. The softening of a flat optic branch will therefore force the acoustic mode branch to soften to a greater extent as $\boldsymbol{k}$ increases, leading to a complete softening to zero frequency at an

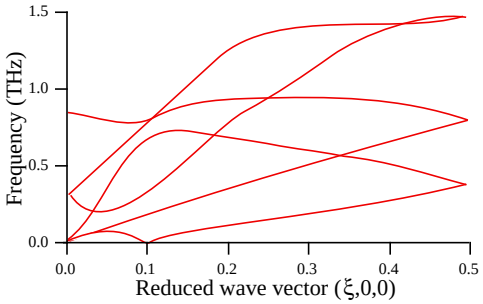

Figure 5. Calculated dispersion curves along $(1, 0, 0)$ for α-ZrW_2O_8 at 1.53 GPa showing the soft mode at the wavevector $\boldsymbol{k} \sim \boldsymbol{a}^*/10$.

incommensurate wavevector.

With further increasing pressure, the branch softens for a wider range of wavevectors, including $\boldsymbol{k} = \boldsymbol{a}^*/3$. At 2 GPa, the structure which results when the soft mode at $\boldsymbol{a}^*/3$ 'freezes-in' has a lattice enthalpy 0.24 eV per formula unit lower than that of cubic α-ZrW_2O_8 but only marginally larger, 0.01 eV per formula unit, than γ-ZrW_2O_8. While this phase is not expected to materialize in ZrW_2O_8, the marginal energy difference which prevents its formation may be overcome in an analogue material and the displacive instability would then become important.

4.2. Reconstructive instability

Further application of pressure to α-ZrW_2O_8 in our model caused a reconstructive phase transition to a structure with sevenfold coordinated zirconium atoms, which we denote as α'-ZrW_2O_8. Figure 2 and table 4 show the crystal structure of α'-ZrW_2O_8 at 7 GPa. It can be seen that the tungsten atoms have remained fourfold coordinated. The critical pressure P_0 for the α'–γ transition was calculated as 1.56 GPa and the associated change in lattice energy was 0.19 eV per formula unit. The increased coordination of the zirconium atoms in α'-ZrW_2O_8 causes a substantial volume contraction resulting in a volume difference of 11% between α'- and γ-ZrW_2O_8.

It is interesting to note that we have calculated a positive coefficient of thermal expansion for our hypothetical α'-ZrW_2O_8 of 8.7×10^{-6} K^{-1}, and a bulk modulus of 1.04×10^{-2} GPa^{-1} that is about twice as large as that of α'- and γ-ZrW_2O_8.

While we may not be able to predict that there will not be some other phase with a yet still lower energy, we can note the result that increasing pressure is more likely to result in distortions of the ZrO_6 octahedra than the WO_4 tetrahedra, and any high-pressure phase is likely to retain the WO_4 tetrahedra in its structure but may lose the ZrO_6 octahedra. Distortions of the ZrO_6 octahedra will indeed give a mechanism for any high-pressure reconstructive phase transition.

5. Summary

The observation of a new high-pressure phase in ZrW_2O_8 which also has negative thermal expansion has enabled us to confirm the mechanism we described earlier to explain the negative thermal expansion in α-ZrW_2O_8. It has also provided an opportunity to validate our model inter-atomic potentials thereby gaining insight on the crystal chemistry of γ-

Table 4. Comparison of calculated crystal structures of α-ZrW_2O_8 and α'-ZrW_2O_8 (experimental data obtained at ambient pressure and temperature, calculations correspond to $T = 0$ K and $P = 0$ GPa).

	α-ZrW_2O_8	α'-ZrW_2O_8
a (Å)	9.054	8.602
x (Zr)	0.0093	0.0214
x (W1)	0.3324	0.2889
x (W2)	0.5879	0.5470
x (O1)	0.2062	0.1534
y (O1)	0.4374	0.3512
z (O1)	0.4375	0.4292
x (O2)	0.7748	0.7416
y (O2)	0.5532	0.4871
z (O2)	0.5582	0.5405
x (O3)	0.4783	0.4321
x (O4)	0.2212	0.1667
Zr–O (Å)	3 × 2.086, 3 × 2.113	3 × 2.128, 3 × 2.142, 2.165
W1–O (Å)	1.744, 3 × 1.764, (2.288)	3 × 1.762, 1.820, (2.134)
W2–O (Å)	1.719, 3 × 1.742	1.712, 3 × 1.752

ZrW_2O_8. We have concluded that the WO_4 tetrahedra remain fourfold coordinated and that oxygen atoms from different polyhedra in the structure become more impacted rather than forming additional cross-bracing bonds. We suggest that this impaction is the origin of the observed relative magnitudes of the thermal expansion coefficient and bulk modulus in γ-ZrW_2O_8 both of which are inconsistent with the picture in which cross-bracing bonds have been formed.

As an aside we have described possible instabilities in α-ZrW_2O_8 under pressure which may be of importance in analogue materials and in so doing gained the insight that the ZrO_6 octahedra are more liable to distort and change coordination than the WO_4 tetrahedra in the structure.

Acknowledgments

AKAP is grateful to NERC (UK) for the award of a research studentship. We are pleased to acknowledge the help of Kenton Hammonds (Cambridge) and Julian Gale (Imperial College).

References

[1] Mary T A, Evans J S O, Vogt T and Sleight A W 1996 Negative thermal expansion from 3 to 1050 kelvin in ZrW_2O_8 *Science* **272** 90–2

[2] Pryde A K A, Hammonds K D, Dove M T, Heine V, Gale J D and Warren M C 1996 Origin of the negative thermal expansion in ZrW_2O_8 and ZrV_2O_7 *J. Phys.: Condens. Matter* **8** 10 973–82

[3] Pryde A K A, Hammonds K D, Dove M T, Heine V, Gale J D and Warren M C 1997 Rigid units and the negative thermal expansion in ZrW_2O_8 *Phase Transitions* **61** 141–53

[4] Dove M T, Heine V and Hammonds K D 1995 Rigid unit modes in framework silicates *Mineral. Mag.* **59** 629–39

[5] Hammonds K D, Dove M T, Giddy A P, Heine V and Winkler B 1996 Rigid unit phonon modes and structural phase transitions in framework silicates *Am. Mineral.* **81** 1057–79

[6] Heine V, Welche P R L and Dove M T 1998 Geometrical origin and theory of negative thermal expansion in framework structures *J. Am. Ceram. Soc.* at press

[7] Welche P R L, Heine V and Dove M T 1998 Negative thermal expansion in beta-quartz *Phys. Chem. Minerals* at press
[8] Phillips J C 1979 Topology of covalent non-crystalline solids I: short range order in chalcogenide alloys *J. Non-Cryst. Solids* **34** 153–81
[9] Thorpe M F 1983 Continuous deformations in random networks *J. Non-Cryst. Solids* **57** 355–70
[10] Maxwell J C 1864 On the calculation of the equilibrium and stiffness of frames *Phil. Mag.* **27** 294–99
[11] Giddy A P, Dove M T, Pawley G S and Heine V 1993 The determination of rigid unit modes as potential soft modes for displacive phase transitions in framework crystal structures *Acta Crystallogr.* A **49** 697–703
[12] Hammonds K D, Bosenick A, Dove M T and Heine V 1998 Rigid unit modes in crystal structures with octahedrally-coordinated atoms *Am. Mineral.* **83** 476–9
[13] Evans J S O, Hu Z, Jorgensen J D, Argyriou D N, Short S and Sleight A W 1997 Compressibility, phase transitions and oxygen migration in zirconium tungstate, ZrW_2O_8 *Science* **275** 61–5
[14] Sanders M J, Leslie M and Catlow C R A 1984 Interatomic potentials for SiO_2 *J. Chem. Soc.: Chem. Commun.* 1271–3
[15] Winkler B, Dove M T and Leslie M 1991 Static lattice energy minimization and lattice dynamics calculations on minerals using three-body potentials *Am. Mineral.* **76** 313–31
[16] Gale J D 1997 GULP: A computer program for the symmetry-adapted simulation of solids *J. Chem. Soc.: Faraday Trans.* **93** 629–37
[17] Dove M T 1993 *Introduction to Lattice Dynamics* (Cambridge: Cambridge University Press)
[18] Hammonds K D, Dove M T, Giddy A P and Heine V 1994 CRUSH: A FORTRAN program for the analysis of the rigid unit mode spectrum of a framework structure *Am. Mineral.* **79** 1207–9
[19] Details about the CRUSH program, and copies for general distribution, can be found on `http://www.esc.cam.ac.uk/mineral_sciences/crush`
[20] Hammonds K D, Deng H, Heine V and Dove M T 1997 How floppy modes give rise to adsorption sites in zeolites *Phys. Rev. Lett.* **78** 3701–4
[21] Hammonds K D, Heine V and Dove M T 1997 Insights into zeolite behaviour from the rigid unit mode model *Phase Trans.* **61** 155–72
[22] Hammonds K D, Heine V and Dove M T 1998 Rigid unit modes and the quantitative determination of the flexibility possessed by zeolite frameworks *J. Phys. Chem.* B **102** 1759–67
[23] Vallade M, Berge B and Dolino G 1992 Origin of the incommensurate phase of quartz: II. Interpretation of inelastic neutron scattering data *J. Physique I* **2** 1481–95
[24] Tautz F S, Heine V, Dove M T and Chen X 1991 Rigid unit modes in the molecular dynamics simulation of quartz and the incommensurate phase transition *Phys. Chem. Minerals* **18** 326–36